Homoclinic tangencies, generating partitions and curvature of invariant manifolds

1991 J. Phys. A: Math. Gen. 24 1837

(http://iopscience.iop.org/0305-4470/24/8/024)

J. Phys. A: Math. Gen. 24 (1991) 1837-1887. Printed in the UK

Homoclinic tangencies, generating partitions and curvature of invariant manifolds

Franco Giovannini and Antonio Politi

Istituto Nazionale di Ottica, I-50125 Firenze, Italy

Received 30 July 1990, in final form 30 November 1990

Abstract. A method to compute the curvature of the unstable manifold is introduced and applied to Hénon map and Duffing attractor, showing that it allows us to locate the homoclinic tangencies and, in turn, to construct a generating partition. The probability distribution of curvature-values is investigated, showing a power-law decay. Finally, the shape of the multifractal spectrum of effective Liapunov exponents in non-hyperbolic systems is discussed.

1. Introduction

Knowledge of the evolution in the tangent space of a dynamical system allows one to characterize the chaotic properties of strange attractors in a quantitative way. Simple algorithms have been devised in the past years to compute the characteristic Liapunov exponents (Benettin *et al* 1980, Shimada and Nagashima 1979), from which an almost complete information on metric properties of a chaotic evolution can be extracted.

In this paper we go one step further in the local analysis of stable and unstable manifolds, by determining not only the tangent (i.e. Liapunov) vectors, but also the curvature. Knowledge of this second-order indicator is very useful at least in two instances: accurate estimates of sections of a given strange attractor, and determination of homoclinic tangencies (HT). Moreover, we show that it is possible to extract accurate informations on the non-hyperbolic phase of Hénon-type maps, from the analysis of the tail of the probability distribution of curvature-values. In fact, by rephrasing the argument used below to explain the power-law decay of the probability density (section 3), we modify a previous conjecture raised in Grassberger *et al* (1988) on the shape of the multifractal spectrum of effective (finite-time) Liapunov exponents at small enough values. More precisely, we expect the straight-line behaviour to be substituted, below a critical value λ_c, by a nonlinear curve describing the non-hyperbolic phase (see section 4).

According to Grassberger and Kantz (1985), the determination of HTs allows one to construct a generating partition for a typical non-hyperbolic attractor characterized by a stretch-and-fold dynamics. The main method which has been so far developed to detect HTs requires to determine a periodic orbit belonging to the attractor and its eigenvectors. By then following the expanding direction in the nonlinear regime, one has to look for those points such that infinitesimal distances along the unstable manifold are in fact contracted. Here, starting from the observation that, if a point lies on an HT, then the curvature around its forward iterates must diverge, we introduce an alternative procedure to detect HTs based on the determination of points with high curvature-values.

0305-4470/91/081837+12$03.50

Thanks also to the introduction of Poincaré sections, much progress has been made in understanding the behaviour of 3D flows, with the possibility to generate a 2D image of the invariant measure. However, already the introduction of one extra dimension (4D flows, 3D maps) almost ruins the usefulness of a Poincaré section. In order to take a further section of the attractor (transversal to the unstable manifold), one is forced to compute a huge amount of data points discarding those lying too far from the chosen section, and the inaccuracy on the remaining points can be still non-negligible. An improvement can be obtained by correcting the coordinates of the points from the knowledge of the local direction of the unstable manifold (along which one can certainly find points of the attractor) (Kostelich and Yorke 1986, Badii and Politi 1986). It therefore becomes clear that knowledge of the curvature allows one to make better (second-order) extrapolation on the intersection of the invariant manifold with the chosen surface. While leaving the implementation of such an algorithm to future work, here we focus our attention on the more fundamental problem of determining HTs.

It is important to notice that local curvature values do depend on the coordinates and on the metric chosen to represent a given dynamics. Nevertheless, this is not a real drawback insofar as our main results deal with the case of diverging curvatures. In fact, homoclinic tangencies being strictly associated with infinite curvatures can be unambiguously identified, since any smooth change of coordinates can lead to a finite multiplicative correction only.

Let us start by defining the machinery to compute the local curvature of a manifold. Given a curve Γ in the plane, we can locally parametrize it around a generic point (z_1, z_2) as

$$x_i(t) = z_i + u_i t + p_i \frac{t^2}{2} + O(t^3) \tag{1.1}$$

for $i = 1, 2$. If $\boldsymbol{f} \equiv (f_1(\boldsymbol{x}), f_2(\boldsymbol{x}))$ (with a standard vector notation) is a transformation of the plane onto itself, by applying $\boldsymbol{f}$ to the curve Γ, we obtain a new curve Γ' which can be parametrized in the same way

$$x_i'(t) = z_i' + u_i' t + p_i' \frac{t^2}{2} + O(t^3) \tag{1.2}$$

(for $i = 1, 2$). In order to determine the relations linking the new with the old coefficients, it is sufficient to note that $x_i'(t) = f_i(\boldsymbol{x}(t))$ and then to expand $\boldsymbol{x}'(t)$ in a Taylor series around $t = 0$,

$$x_i'(t) = z_i' + \frac{\partial f_i}{\partial x_j} u_j t + \left(\frac{\partial f_i}{\partial x_j} p_j + \frac{\partial^2 f_i}{\partial x_j \, \partial x_h} u_j u_h \right) \frac{t^2}{2} \tag{1.3}$$

where the summation over repeated indices is, as usual, neglected. By identifying the coefficients in (1.3) with those of (1.2) we find

$$u_i' = \frac{\partial f_i}{\partial x_j} u_j \tag{1.4}$$

whose iteration describes the well known evolution in tangent space of the map $\boldsymbol{f}$, and

$$p_i' = \frac{\partial f_i}{\partial x_j} p_j + \frac{\partial^2 f_i}{\partial x_j \, \partial x_h} u_j u_h \tag{1.5}$$

giving the information about the curvature of the unstable manifold, provided that the vector $\boldsymbol{u}$ already converged to the right direction. In fact, we can recall that the curvature C of a curve Γ given in a parametric form is

$$C = \frac{|\ddot{x}_2\dot{x}_1 - \ddot{x}_1\dot{x}_2|}{(\dot{x}_1^2 + \dot{x}_2^2)^{3/2}} \tag{1.6}$$

where the dot indicates derivative with respect to the parameter t. Accordingly, from expression (1.1),

$$C = \frac{|p_2u_1 - p_1u_2|}{(u_1^2 + u_2^2)^{3/2}}. \tag{1.7}$$

As (1.7) is independent of the parametrization adopted, and being also convenient, during the numerical simulations, to keep the modulus of $\boldsymbol{u}$ constant, the expression of the curvature can be simplified by referring to a unitary vector,

$$C = |p_2u_1 - p_1u_2|. \tag{1.8}$$

2. Hénon map: numerical results

In this section we apply the machinery previously defined to the case of the Hénon map

$$x_{n+1} = 1 - ax_n^2 + by_n \qquad y_{n+1} = x_n. \tag{2.1}$$

The evolution in the tangent space is described by

$$u_{n+1} = -2ax_nu_n + bv_n \qquad v_{n+1} = u_n \tag{2.2}$$

while the second-order corrections evolve according to

$$p_{n+1} = -2ax_np_n + bq_n - 2au_n^2 \qquad q_{n+1} = p_n \tag{2.3}$$

where the notations introduced in the previous section have been, for sake of simplicity, slightly modified. The results of a numerical simulation with the typical parameter values ($a = 1.4$ and $b = 0.3$) are shown in figure 1, where the probability to detect a

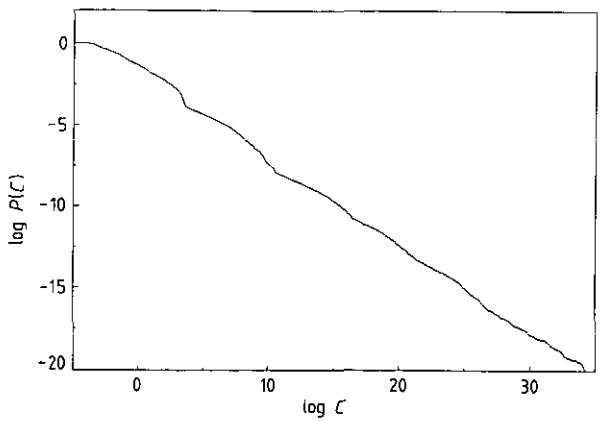

Figure 1. Log–log plot of the probability of detecting a curvature value larger than C, versus C, for the Hénon map with $a = 1.4$ and $b = 0.3$.

curvature-value larger than C is plotted in a log-log scale indicating a clear-cut power-law decay

$$P(C) \simeq C^{-\alpha} \tag{2.4}$$

at large C, with $\alpha \simeq 0.57$. The empirical relation (2.4) will be justified in the next section, where we also express α in terms of the characteristic Liapunov exponents.

In figure 2(b), we show a sequence of expanding (continuous line) and contracting (dashed line) single-step multipliers, while in figure 2(a) a few iterates of the curvature of the stable (dashed line) and unstable (continuous line) manifold are drawn. The two dashed curves have been obtained by inverting equations (2.2) and (2.3) and using the inverse of the same orbit computed forward in time, as a reference trajectory. It is clearly seen that, when the curvature of the unstable manifold is increasing up to a local maximum, the two multipliers do coincide, indicating that the two invariant manifolds are nearly tangent. Moreover, we can also notice that before the curvature peak of the unstable manifold, a curvature peak of the stable manifold is observed as well, confirming that the concept of 'primary' HT, as the point where the sum of the curvatures of the two manifolds is minimum (along each sequence of tangencies), at least makes sense from a numerical point of view. We indeed recall that the suggested construction of a generating partition is based on the idea of connecting all primary tangencies by a dividing line. In this case we confirm that the minima, identified from all sequences yielding a large peak of the curvature, correspond to the points lying on the border of the partition, as from Grassberger and Kantz (1985). We return to this point in section 5, when analysing the Duffing attractor.

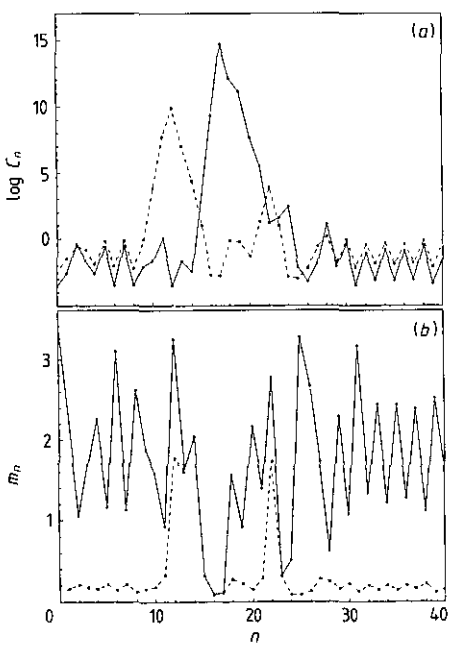

Figure 2. (a) Curvature of stable (broken curve) and unstable (full curve) manifold along an orbit passing close to an HT; (b) forward (full) and backward (broken) single-step multipliers along the same orbit.

3. Probability distribution of curvatures

Here, we justify (2.4) following two complementary approaches: a geometric one, starting from the knowledge of the structure of the Hénon attractor, and an analytic one, based on the recursive equation satisfied by the curvature.

We start from the observation made in the last part of the previous section that large curvatures can only be detected in the vicinity of the iterates of primary HTs. Following the approach devised in Politi *et al* (1988), to characterize the non-hyperbolic phase of the Hénon attractor, we approximate the unstable manifold in the neighbourhood of a primary tangency with the parabola

$$y = x^2. \tag{3.1}$$

The nth iterate of such a parabola is

$$y_n = e^{(B-3\lambda_0)n} x_n^2 \tag{3.2}$$

where we have assumed a contraction rate equal to $e^{\lambda_0 n}$ along the x axis and an expansion $e^{(B-\lambda_0)n}$ along the y direction (with $B = \log b$).

The curvature of parabola (3.2) is maximum in correspondence of its vertex, where it is

$$D_n = e^{(B-3\lambda_0)n} \tag{3.3}$$

where an irrelevant factor 2 has been omitted. To estimate the probability $P(C)$ to find a curvature value larger than C, we first need to determine the minimum number of iterates $n(C)$ necessary to have D_n large enough. From (3.3) we obtain

$$n(C) = \frac{\log C}{B - 3\lambda_0}. \tag{3.4}$$

For $n > n(C)$ there is an interval of width δx_n around the tangency, where the curvature remains larger than C. From relation (1.6) and equations (3.2) and (3.3) we can determine the curvature around a point distant δx_n,

$$C = \frac{y''}{(1+y'^2)^{3/2}} = \frac{D_n}{(1+D_n^2 \delta x_n^2)^{3/2}} \tag{3.5}$$

where the prime indicates the derivative with respect to x. By solving for δx_n, we obtain

$$\delta x_n = \frac{1}{D_n} \sqrt{\left(\frac{D_n}{C}\right)^{2/3} - 1}. \tag{3.6}$$

The second addendum under the square root can be neglected, thus obtaining

$$\delta x_n \simeq (D_n^2 C)^{-1/3}. \tag{3.7}$$

By mapping the nth iterate of the HT back to the primary tangency, the width δx_0 is determined:

$$\delta x_0 = C^{-1/3} e^{(\lambda_0 - 2B/3)n}. \tag{3.8}$$

By further assuming that the Hénon attractor is essentially smooth along the unstable manifold (see also Politi *et al* 1988), and neglecting the dependence of λ_0 on the HT, we have that the probability of detecting a curvature-value larger than C around an

nth order HT is of the same order as δx_0. Accordingly, the global probability $P(C)$ is obtained by summing over all admissible n (i.e. larger than $n(C)$):

$$P(C) \simeq C^{-1/3} \sum_n e^{(\lambda_0 - 2B/3)n}. \tag{3.9}$$

The coefficient $(\lambda_0 - 2B/3)$ is less than 0 for the typical value of the negative Liapunov exponent, so that the scaling behaviour at large C-values is controlled by the smallest admissible n value. A simple substitution of (3.4) yields

$$\alpha = \frac{B - 2\lambda_0}{B - 3\lambda_0}. \tag{3.10}$$

By considering $\lambda_0 = -1.61$ (i.e. the value of the negative Liapunov exponent), we obtain $\alpha = 0.556$ which is in reasonable agreement with the result of direct simulations ($\simeq 0.57$). The discrepancy is probably to be ascribed to the fact we have neglected the fluctuations of λ_0 associated with the multifractal structure of the hyperbolic phase of the Hénon attractor.

Let us now pass to the second approach. From (1.7) and (2.3) we obtain the following recursive relation for the curvature:

$$C_{n+1} = -\frac{bC_n}{m_{n+1}^3} + \frac{2au_n^3}{m_{n+1}^3} \tag{3.11}$$

where the curvature is taken with sign, m_{n+1} denotes the single-step multiplier value, and u_n is referred to a unitary vector. Being interested only in the statistics of large C-values, we can neglect the second term in the RHS of (3.11). It is only relevant in preventing C_n from becoming exceedingly small. By further introducing $S_n = \log|C_n|$, we find

$$S_{n+1} = (B - 3\lambda_n) + S_n \tag{3.12}$$

which describes a diffusive motion (with drift, as well) on a line with a reflecting barrier put at $S = 0$ simulating the effect of the term we have neglected. As most of the probability distribution of S is concentrated around $S = 0$, and from the definition of effective Liapunov exponent as the expansion rate over n time steps, we have

$$S_n = (B - 3\lambda)n. \tag{3.13}$$

In other words the probability distribution of large S is the same as that of small λ, apart from a rescaling of variables. Accordingly, (3.13), showing the equivalence between the evolution of effective Liapunov exponents and that of large curvatures, confirms the independence of the expected scaling law (2.4) on the choice of the coordinates. By recalling that

$$P(\lambda; n) \simeq e^{-g(\lambda)n} \tag{3.14}$$

we have, from (3.13),

$$P(S; n) \simeq \exp\left[-g\left(\frac{B - S/n}{3}\right)n\right]. \tag{3.15}$$

Being interested in the negative λ tail of the distribution, let us recall that, from Grassberger *et al* (1988),

$$g(\lambda) = K_2 - \lambda \tag{3.16}$$

where K_2 is the generalized metric entropy K_q of order 2. Upon substituting (3.16) in (3.15) we have

$$P(S; n) \simeq \exp[(B/3 - K_2)n - S/3]. \tag{3.17}$$

Since $(B/3 - K_2) < 0$, the scaling behaviour of the probability summed over all n values is obtained for n as small as possible. From (3.13) we can determine such n from the knowledge of S and of $\lambda_{\min}$

$$n_0 = \frac{S}{B - 3\lambda_{\min}}. \tag{3.18}$$

Substitution in (3.17) yields

$$\alpha = \frac{K_2 - \lambda_{\min}}{B - 3\lambda_{\min}}. \tag{3.19}$$

By substituting $\lambda_{\min}$ with the most probable value of the Liapunov exponent we obtain a result which is slightly smaller than the previous one obtained from (3.10) ($\alpha = 0.54$). In this case, the crucial approximation behind the derivation of (3.19) is the choice of the proper $\lambda_{\min}$ value, a problem equivalent to determining the negative-λ tail of $g(\lambda)$, which was solved in Grassberger *et al* (1988) by conjecturing (3.16). In the next section we return to this question by rephrasing the first approach here applied to determine the scaling behaviour of $P(C)$.

4. Multifractality of the Liapunov spectrum

Here, we discuss the validity of the conjecture raised in Grassberger *et al* (1988) on the existence of a first-order phase transition in the spectrum of the first Liapunov exponent in Hénon-type maps. In fact, we show that the straight line behaviour of $g(\lambda)$ does not proceed down to the smallest value of the first Liapunov exponent. A new highly non-trivial non-hyperbolic phase is expected in the last part of the spectrum.

In order to estimate the probability of finding a Liapunov exponent smaller than λ we again refer to the nth iterate of a primary tangency. The multiplier is computed by determining the expansion (contraction) rate along the tangent to the unstable manifold. One straightforwardly obtains

$$e^{\lambda n} = e^{\lambda_0 n} \sqrt{\frac{1 + 4\, e^{2(B - 2\lambda_0)n} x^2}{1 + 4x^2}} \tag{4.1}$$

for a point at distance x from a primary tangency. As $\lambda > \lambda_0$ and $(B - \lambda_0) > \lambda$, we can neglect the '1' and $4x^2$ terms above and below the sign of fraction, respectively. By further solving for x we obtain

$$x = e^{(\lambda + \lambda_0 - B)n}. \tag{4.2}$$

The smoothness of the attractor along the unstable manifold suggests that the probability of finding an effective Liapunov exponent smaller than λ (i.e. a point closer than x to a primary tangency) is of the same order as x itself times the probability of finding λ_0. In the following, rather than referring to λ_0, we prefer to introduce $\lambda_+ \equiv B - \lambda_0$ which we conjecture to be distributed as the positive Liapunov exponent in the hyperbolic phase. Accordingly, we find

$$P(\lambda, \lambda_+; n) = e^{(\lambda - \lambda_+ - g(\lambda_+))n}. \tag{4.3}$$

The value of $P(\lambda; n)$ is finally obtained by taking the maximum over all possible λ_+. This is obtained for

$$g'(\lambda_+^*) = -1 \tag{4.4}$$

which, from the theory of multifractal sets, yields

$$\lambda_+^* + g(\lambda_+^*) = K_2 \tag{4.5}$$

which confirms (3.16). However, we must notice that, for λ sufficiently negative, λ_+ cannot take the critical value λ_+^*. Indeed, we must recall that

$$\lambda_+ \geqslant B - \lambda. \tag{4.6}$$

This means that there is a critical value

$$\lambda_c = B - \lambda_+^* \tag{4.7}$$

below which (3.16) can no longer hold. In other words it appears very plausible that the straight-line behaviour of the Liapunov spectrum is confined between λ_c and λ_+^*. For $\lambda < \lambda_c$ the maximum over all possible λ_+-values is attained just for the smallest possible value of λ_+, which is obtained when the equality holds in (4.6). By substituting in (4.3), we obtain the expression

$$g(\lambda) = B - 2\lambda + g(B - \lambda) \tag{4.8}$$

which holds for $(B - (\lambda_+)_{max}) < \lambda < \lambda_c$, where the minimum λ-value is obtained in correspondence of the largest λ_+. A semi-quantitative picture of $g(\lambda)$ is presented in figure 3 with the three different phases: (*a*) the non-hyperbolic region, where the multifractality of homoclinic tangencies prevails; (*b*) a straight-line behaviour indicating a first-order phase transition in the generalized Liapunov exponents; (*c*) the usual hyperbolic phase.

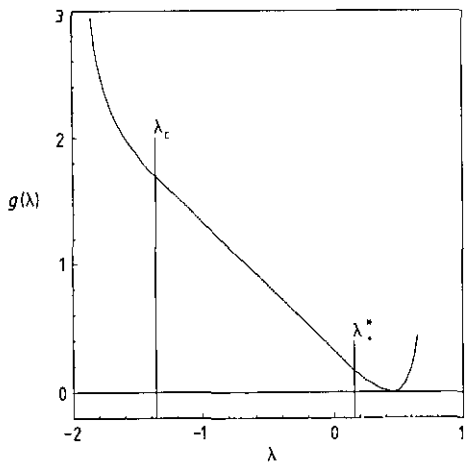

Figure 3. Spectrum $g(\lambda)$ of the effective positive Liapunov exponent for the Hénon map. The expected three different regimes are reported: hyperbolic phase above λ_+^*; non-hyperbolic phase below λ_c; intermediate region characterized by a straight-line behaviour in between.

5. Generating partition of Duffing attractor

In section 2 we have seen that the choice of points with high curvature values really allows us to pick up the HTs. According to the conjecture raised in Grassberger and Kantz (1985), such points represent the ingredient necessary to build a generating partition. The main remaining problem is the choice of the correct point in any doubly infinite sequence of tangencies. It was conjectured that the relevant tangencies, called 'primary', are those where the sum of the curvatures of stable and unstable manifold is minimum. In section 2 we have confirmed such an hypothesis for the Hénon map with the usual parameter values. In this section we study a flow, namely the Duffing oscillator,

$$\dot{x} = y \qquad \dot{y} = -\delta y + x - x^3 + \gamma \cos ft \tag{5.1}$$

to further check the correctness of this conjecture and also to determine for the first time a non-trivial generating partition for a flow (in the Lorenz model, there is no folding and thus the problem does not appear at all; in some cases, the partition can be determined from symmetry considerations only (Shimada 1979, otherwise see Badii *et al* 1990)).

The arguments used in the introduction to determine the evolution equations of the curvature in a recursive map need to be repharased for a flow. The main difference is the existence of an extra direction to be taken into account. However, for a periodically forced system like Duffing attractor, the extra component of the Liapunov vector is constant and thus irrelevant. It is straightforwardly seen that the same machinery applied to the RHS of map (2.1) has now to be referred to the RHS of flow (5.1). The equations for the evolution in the tangent space are

$$\dot{u} = v \qquad \dot{v} = (1 - 3x^2)u - \delta v \tag{5.2}$$

and those for the second-order terms,

$$\dot{p} = q \qquad \dot{q} = (1 - 3x^2)p - \delta q - 6xu^2. \tag{5.3}$$

They have been numerically integrated for $\delta = 0.25$, $f = 1$ and $\gamma = 0.4$ (values where a strange attractor is likely to exist, as from Guckenheimer and Holmes (1983). An image of a Poincaré section, taken when the phase of the forcing term is a multiple of 2π, is presented in figure 4. In practice, the symmetry of the attractor allowed us to cut the return time to the Poincaré section by a factor 2, by adding the points where the phase of the forcing term is any multiple of π. In fact, from (5.1), it is immediately seen that, upon changing x and y in $-x$, $-y$, respectively, the flow equations remain unchanged, provided that the sign of the forcing term is changed as well. Therefore, formally speaking, the attractor shown in figure 4 can be interpreted as arising from an integration of equation (1) over half a period plus the inversion of the sign of its coordinates.

The dots in figure 4 denote the HTs which pertain the definition of a generating partition. They have been determined by first looking for peaks of the curvature of the unstable manifold (in a very long trajectory), by further determining the closest minimum of the sum of curvatures occurring before the peak, plus a final 'adjustment' (see below). In figure 5 we present the results equivalent to those for the Hénon map shown in figure 2. Again, we can observe that whenever the curvature $C(t)$ becomes very high, the forward and backward expansion rates are almost the same, indicating that stable and unstable manifolds are tangent to each other. The structure of the

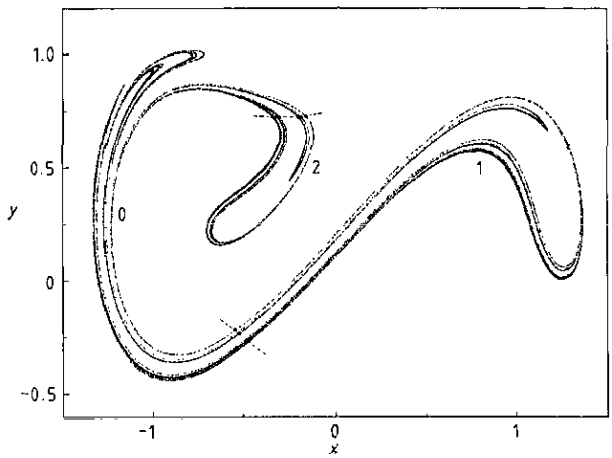

Figure 4. Poincaré section of Duffing attractor and the three-symbol generating partition.

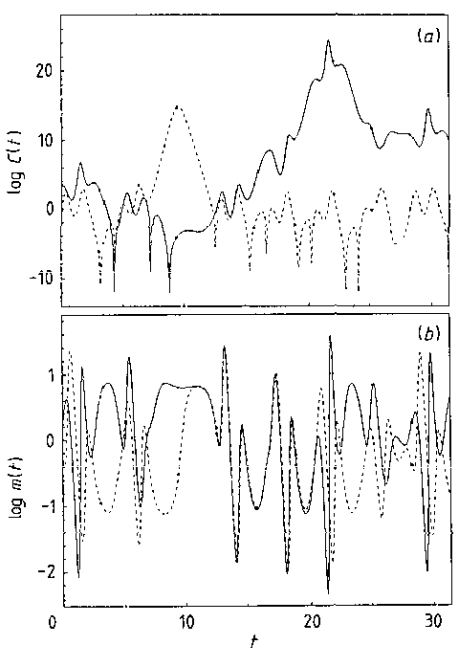

Figure 5. (*a*) Evolution of the curvature of stable and unstable manifold (broken and full curve, respectively) around an HT of the Duffing attractor. (*b*) Evolution of positive and negative expanding rates (full and broken curve, respectively) along the same trajectory as in (*a*).

attractor is clearly split into three parts from such tangencies so that we are led to introduce three symbols (see figure 4). In order to check that this is really a generating partition, we have computed the Kolmogorov-Sinai entropy K_1 and compared it with the Liapunov exponent. By interpreting each string of symbols as the ternary expansion of a number between 0 and 1, we could then estimate K_1 by using a standard algorithm to compute the information dimension. More precisely, we have used the nearest-neighbour algorithm (Badii and Politi 1984), which was shown to be more effective in

Grassberger (1989) and Grassberger and Fahner (1987). (The presence in our case of three symbols makes the determination of block entropies more involved than usual.) The results are presented in figure 6 for two different orders of neighbours (namely 4 and 20), showing a nice convergence to the Liapunov exponent $\lambda = 0.1567$.

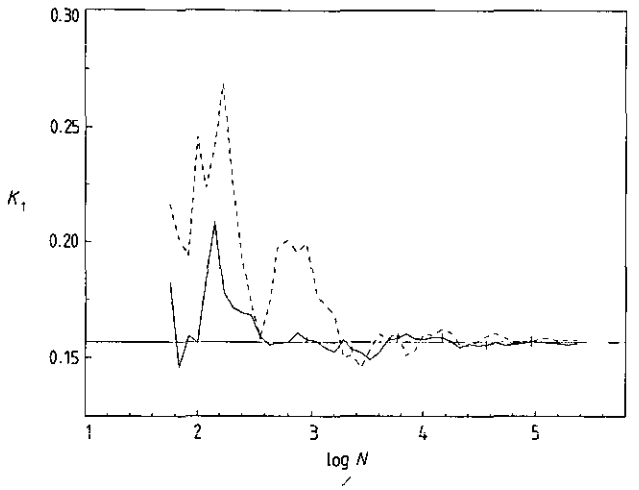

Figure 6. Kolmogorov-Sinai entropy computed with a nearest-neighbour method versus the number of points. Full and broken curves refer to the 4th and 20th neighbours. The horizontal line refers to the Liapunov exponent $\lambda \simeq 0.1567$.

Let us also make a remark about the unusually high 'multifractality' of this strange attractor. In comparison with the Kolmogorov-Sinai entropy $K_1 \simeq 0.157$, the topological entropy K_0 is around 0.25! In fact, we have only found the following list of irreducible forbidden sequences: 02 and 22 of length 2, 2121 of length 4, 00000 and 20000 of length 5, 000010, 000011, 010000, 012000, 200010, and 212012 of length 6. We could not go to much longer blocks because of the exceedingly small probability of some sequences. By constructing a graph for his grammar and computing the topological entropy as the largest eigenvalue of its adjacency matrix (Crutchfield and Young 1989, Isola and Politi 1990), we obtain $K_0 = 0.266$, but the convergence appears very slow and the second digit is already unreliable.

We have good numerical evidence that the partition shown in figure 4 is indeed a generating one. Going back to the HTs which define it, it is no longer true (as for the Hénon map) that each such tangency corresponds to the minimum of the sum of the curvatures: in some cases it corresponds to the next or to the previous iterate. Therefore, we must conclude that the concept of 'primary' tangency remains vaguely defined. This is not surprising, by recalling that finite curvature values do depend on the choice of the coordinates, so that the point with minimal curvature may not be invariant under change of variables.

This is not a problem at all if one is interested in determining scaling laws as in sections 3 and 4 of the present paper; however, it makes the definition of generating partition not completely 'automatic'. For instance, in the case of Duffing attractor, we have been able to identify the relevant tangencies, by determining the largest compact subsets of the attractor (delimited by HTs) whose image was not 'folded' on the attractor. Obviously this is a heuristic argument which calls for a necessary refinement.

Acknowledgments

One of us (AP) thanks the Institute for Scientific Interchange (Torino) for the kind hospitality and for the computing facilities offered in connection with the programme on 'Complexity and Evolution', when part of the work was done. We also thank P Grassberger for a careful reading of the manuscript.

References

Badii R, Finardi M and Broggi G 1990 in preparation
Badii R and Politi A 1984 *Phys. Rev. Lett.* **52** 1661
—— 1986 *Proc. Conf. on Dimensions and Entropies in Chaotic Systems* ed G Mayer-Kress (Berlin: Springer)
Benettin G, Galgani L, Giorgilli A and Strelcyn J M 1980 *Meccanica* **15** 9
Crutchfield J P and Young K 1989 *Phys. Rev. Lett.* **63** 105
Grassberger P 1989 *IEEE Trans. Inf. Th.* **35** 3
Grassberger P, Badii R and Politi A 1988 *J. Stat. Phys.* **51** 135
Grassberger P and Fahner G 1987 *Complex Systems* **1** 1093
Grassberger P and Kantz H 1985 *Phys. Lett.* **113A** 235
Guckenheimer J and Holmes P 1983 *Nonlinear Oscillations, Dynamical Systems, and Bifurcations of Vector Fields* (New York: Springer)
Isola S and Politi A 1990 *J. Stat. Phys.* **61** 263
Kostelich E J and Yorke J A 1986 *Proc. Conf. on Dimensions and Entropies in Chaotic Systems* ed G Mayer-Kress (Berlin: Springer)
Politi A, Badii R and Grassberger P 1988 *J. Phys. A: Math. Gen.* **21** L763
Shimada I 1979 *Prog. Theor. Phys.* **62** 61
Shimada I and Nagashima T 1979 *Prog. Theor. Phys.* **61** 1605